AN IMMERSED BOUNDARY METHOD BASED ON THE KINEMATIC RELATION OF THE VELOCITY-VORTICITY FORMULATION

I. Farahbakhsh H. Ghassemi *

Department of Ocean Engineering
Amirkabir University of Technology
Tehran, Iran

F. Sabetghadam

Mechanical and Aerospace Engineering Department
Science and Research Branch
Islamic Azad University
Tehran, Iran

ABSTRACT

An immersed boundary method is proposed for the simulation of the interaction of an incompressible flow with rigid bodies. The method is based on a new interpretation of velocity-vorticity formulation and no longer includes the force term which is an essential issue of common immersed boundary methods. The system is considered in an Eulerian frame and retrieving the vorticity in this formulation enforces continuity at the fluid-solid interface and rigid motion of the solid. The method focuses on the mutual kinematic relations between the velocity and vorticity fields and with retrieving the vorticity field and re-calculating the velocities yields the solenoidal velocity field. The method is applied to the two dimensional problems and the results show that the solenoidality is satisfied acceptably. The comparisons with 2D test cases are provided to illustrate the capabilities of the proposed method.

Keywords: Velocity-vorticity formulation, Immersed boundary method, Incompressible flow, Solenoidal velocity field.

1. INTRODUCTION

The numerical solution of the equations which govern the dynamics of fluid as a continuum are encountered some difficulties when the boundary conditions was not being set properly [1,2]. These equations that express conservation of mass and momentum, Navier-Stokes equations, are derived to model the phenomena in principal physical domain. When a computational domain is selected to be cut from the physical domain, non-physical solution may be obtained due to improper implementation of boundary conditions. This issue is very vital in primitive and secondary variables formulation of the incompressible Navier-Stokes equations [3,4].

Any type of discontinuities in the computational field (simply-connected or multiply-connected) similarly gives rise to some difficulties especially in incompressible flows as non-solenoidal velocity fields. Hence reaching a divergence-free velocity field is one of the most important topics of almost all algorithms of incompressible flow simulations, either primitive or secondary variables formulations [5]. Although some certain types of boundary conditions are labeled and proven as improper [2], they have widespread use in relevant literature.

In recent years numerous numerical methods are proposed to encounter discontinuities as embedded bodies [6-10]. Immersed boundary method (IBM) which is developed by Peskin [11] has received a lot of attentions in the last few years. In his pioneering work on the investigation of the blood flow in human heart the IBM is proposed which handles the flow field computation around a discontinuity. The IBM facilitates the task of grid generation and uses the Cartesian mesh thanks to applying the singular force on the Lagrangian coordinates of the boundary. Following the vanguard work of Peskin [11], numerous versions of IBM have been developed. Fadlun *et al.* [12] combined immersed boundary and finite-difference methods to simulate the three dimensional complex flows. An immersed boundary finite-volume method was also developed by Kim *et al.* [13] for simulation of the flow in irregular geometries. Griffith [14] represented an adaptive and parallel version of the immersed boundary method to investigate the blood-muscle-valve mechanics of the heart. A penalty immersed boundary method was proposed by Kim and Peskin [15] for simulation of elastic boundaries with mass. For simulating the viscous flows in irregular

* Corresponding author (gasemi@aut.ac.ir)

DOI : 10.1017/jmech.2014.82
Copyright © 2014 The Society of Theoretical and Applied Mechanics, R.O.C.
https://doi.org/10.1017/jmech.2014.82 Published online by Cambridge University Press

domains, Le *et al.* [16] developed an implicit-forcing immersed boundary method. Poncet [17] presented numerical analysis and practical considerations for three-dimensional flow computation using an implicit immersed boundary method. He investigated the Euler equations in their vorticity formulation and context of flow computation around an arbitrarily shaped body. In his work, this is demonstrated that one can use sources of potential velocity field, dispatched on the body, to produce a velocity through this surface, aiming in practice at cancelling a flow-through velocity.

A novel numerical procedure based on the immersed boundary technique was proposed by Bonfigli [18] to solve the incompressible Navier-Stokes equations around complex geometries with fourth-order spatial and temporal accuracy. Ren *et al.* [19] proposed a new stream function-vorticity formulation-based immersed boundary method. Different from the conventional immersed boundary method, the main feature of their model is to accurately satisfy both governing equations and boundary conditions through velocity correction and vorticity correction procedures. The velocity correction process is performed implicitly based on the requirement that velocity at the immersed boundary interpolated from the corrected velocity field accurately satisfies the nonslip boundary condition.

Wu and Young [20] described the numerical investigations of the flow and wave patterns under stationary or moving submerged objects in a viscous fluid. For dealing with complex submerged objects in the fluid, they adopted a hybrid Cartesian/immersed boundary method to allow imposition of the solid boundary conditions with a linear interpolation approach. The considered physical model is developed for incompressible, unsteady free surface flows to satisfy the condition of volume conservation based on the staggered finite-difference spatial discretization.

Immersed boundary method has also received attention in many aspects of engineering, science, biology and their interdisciplinary fields. Uhlmann [21] presented an improved method for computing incompressible viscous flow around suspended rigid particles using a fixed and uniform computational grid. The flow around an arbitrary moving bodies is also simulated by Kim and Choi [22] using the immersed boundary method. Huang *et al.* [23] proposed an improved version of immersed boundary method for simulating flexible filaments in a uniform flow using an efficient Navier-Stokes solver on the basis of the fractional step method and a staggered Cartesian grid system. They defined the fluid and filament motion on an Eulerian and Lagrangian frame, respectively, and calculated the interaction force using a feedback law, explicitly. Zhao *et al.* [24] presented a fixed-mesh algorithm to simulate the flow-structure interactions such as those occurring in biological systems like advected elastic disk, a flexible leaflet in an oscillating flow, and a model of a swimming jellyfish. Le *et al.* [25] presented an implicit immersed boundary method for the incompressible Navier-Stokes equations with the capability of handling three dimensional membrane-fluid flow interactions. A new implicit iterative algorithm was developed by Curet *et al.* [26] to solve the swimming velocities of the organism with predetermined deformation kinematics. Herschlag and Miller [27] used the immersed boundary method to solve the two dimensional Navier-Stokes equations coupled to the motion of a simplified jellyfish. Chaudhuri *et al.* [28] described the implementation of the immersed boundary method using the direct forcing concept to investigate complex shock-obstacle interactions. Their algorithm has more stable boundary conditions with easier implementation procedure. Wang *et al.* [10] also proposed a new immersed boundary method based on velocity-vorticity formulations for the simulation of 2D incompressible viscous flow. They obtained the corrected velocity from the multi-direct forcing to ensure the well satisfaction of the no-slip boundary condition at the immersed boundary.

In this paper the focus is on a new description of the velocity-vorticity formulation and mutual relation between the velocity and vorticity with the exception that the direct forcing is no longer necessary to construct a solenoidal field around the structure domain. Therefore, this method is quite different from the method of Wang *et al.* [10] and the vorticity field is retrieved from the velocity field, which is padded by the velocity of the immersed boundary, and used to generate a solenoidal velocity field. This method, as will be stated in the following sections, is appropriate for generic fluid-structure interaction problems consist moving and stationary bodies with deformable or rigid structure. In the current study the rigid bodies are merely considered and deformable bodies are left as an interesting topic for our next papers.

An outline of the paper is as follows. In section 2 the mathematical framework is described. In section 3, to validate this method and discuss its accuracy, we focus on test cases where quantitative and qualitative comparisons are possible, namely the circular Couette flow, in-line oscillating cylinder in quiescent fluid, Falling a two dimensional cylinder in quiescent fluid and cavity flow with circular obstacles. Finally section 4 is devoted to concluding remarks and perspectives.

2. MATHEMATICAL FRAMEWORK

2.1 Harmonic Functions

Consider $\mathbb{R}^n$ as *n*-dimensional Euclidean space, so that $\mathbb{R}^1$ and $\mathbb{R}^2$ denote the line and plane, respectively. Let $\Omega \subset \mathbb{R}^n$ be a connected open set as a domain. A function $h:\Omega \to \mathbb{R}$ is harmonic if h has continuous second partial derivatives and the sum of the pure second partial derivatives vanishes, *i.e.* $\Sigma_{i=1}^{n} h_{x_i x_i} \equiv 0$.

Harmonic functions have several characteristics, *i.e.*, invariance property, mean value property and maximum principle. In the present study, maximum principle is

https://doi.org/10.1017/jmech.2014.82 Published online by Cambridge University Press

exploited, as a consequence of mean value property to clarify the treatment of the velocity divergence field. Here, the theorem of mean value property is expressed and left without proof and in consequence the theorem of maximum principle is expressed and proved using the previous one.

Theorem 1 (Mean value property)

Consider $B(X,r)=\{x\in\mathbb{R}^n:|x-X|<r\}$ as a open ball with center X and radius r which its closure is defined as closed ball $\overline{B}(X,r)$. If h is harmonic on $\overline{B}(X,r)$, then $h(X)$ equals the average of h over $B(X, r)$, strictly speaking,

$$h(X)=\frac{1}{V\left(B(X,r)\right)}\int_{B(X,r)}hdV\,. \tag{1}$$

Theorem 2 (Maximum principle)

Suppose Ω is connected open set, h is real valued and harmonic on Ω, and h has a maximum or a minimum in Ω. Hence h is constant.

Proof: Suppose h attains a maximum at $X \in \Omega$. Choose $r > 0$ such that $\overline{B}(X,r)\subset\Omega$. If h be less than $h(X)$ at some point of $B(X, r)$, then the continuity of h causes that the average of h over $B(X, r)$ be less than $h(X)$, contradicting the Theorem 1. Therefore h is constant on $B(X, r)$, providing that the set where h attains its maximum is open in Ω. Because this set is also closed in Ω (by the continuity of h), it must be all of Ω (by connectivity). Thus h is constant on Ω, as desired. If h attains a minimum in Ω, we can apply this argument to $-h$.

Corollary 1

Let Ω is bounded and h is a continuous real valued function on $\overline{\Omega}$ that is harmonic on Ω. Hence h attains its maximum and minimum values over $\overline{\Omega}$ on ∂Ω.

The foresaid corollary which is directly inferred from the previous theorem proof is useful for describing that why velocity divergence field attains its maximum value on the boundary.

2.2 Kinematic Velocity-Vorticity Relation

The most straightforward fundamental equations which govern the physics of the incompressible flow are Navier-Stokes equations in well known formulation of the primitive variables which are given by

$$\partial_t \boldsymbol{u}+\boldsymbol{u}.\nabla\boldsymbol{u}=-\nabla p+\nu\Delta\boldsymbol{u}+\boldsymbol{f}\,, \tag{2}$$

$$\nabla.\boldsymbol{u}=0\,, \tag{3}$$

where $x \in \Omega$ is the vector of Cartesian coordinates, Ω is a bounded or unbounded connected open subset of $\mathbb{R}^3$, $\boldsymbol{u}$ is the velocity vector, p is the pressure divided by the constant density ρ of the fluid, $\boldsymbol{f}$ is the body force per unit of mass and ν represents the kinematic viscosity. These set of equations must be completed to properly describe an initial boundary value problem. Therefore, an initial solenoidal condition $\boldsymbol{u}_0$ must be specified as follows

$$\boldsymbol{u}(\boldsymbol{x},t_0)=\boldsymbol{u}_0(\boldsymbol{x})\,,\ \text{where}\ \nabla.\boldsymbol{u}_0=0\,,\ \boldsymbol{x}\in\Omega\,. \tag{4}$$

The boundary conditions

$$\boldsymbol{u}(\boldsymbol{x},t)=\boldsymbol{u}_{\partial\Omega}(\boldsymbol{x},t)\,,\ \boldsymbol{x}\in\partial\Omega \tag{5}$$

must be also applied to satisfy the global mass conservation constraint

$$\oint_{\partial\Omega}\boldsymbol{n}\,.\,\boldsymbol{u}_{\partial\Omega}\,d\sigma=0 \tag{6}$$

on the boundary ∂Ω of the domain, where $\boldsymbol{n}$ is a vector normal to the boundary.

Taking the curl of the momentum equations immediately eliminates the pressure term and results in the vorticity-transport formulation. Boundary conditions must be set in a qualified manner to make this representation equivalent to the primitive variables formulation. To specify a solution, the vorticity-transport equation

$$\partial_t\,\boldsymbol{\omega}+\boldsymbol{u}\,.\,\nabla\boldsymbol{\omega}=\boldsymbol{\omega}\,.\,\nabla\boldsymbol{u}+\nu\Delta\boldsymbol{\omega}+\nabla\times\boldsymbol{f} \tag{7}$$

must be completed by

$$\Delta\boldsymbol{u}=-\nabla\times\boldsymbol{\omega} \tag{8}$$

which is derived with the aid of vorticity vector definition (*i.e.* $\boldsymbol{\omega}=\nabla\times\boldsymbol{u}$), and identity

$$\Delta\boldsymbol{u}=\nabla(\nabla\,.\,\boldsymbol{u})-\nabla\times(\nabla\times\boldsymbol{u}) \tag{9}$$

and use the fact that $\boldsymbol{u}$ is a solenoidal field. The velocity divergence can be scrutinized using the harmonic functions theory. The maximum principle which has been introduced in subsection 2.1, has a essential role in interpreting the divergence of the velocity field. Taking the divergence of the Poisson Eq. (8) results in

$$\Delta(\nabla\,.\,\boldsymbol{u})=0\,, \tag{10}$$

which indicates that the divergence of the velocity is a harmonic function and can not be necessarily zero everywhere. On the basis of Theorem 2 and Corollary 1, velocity divergence is constant over the closure $\overline{\Omega}$ or else attains its maximum and minimum values over the closure domain $\overline{\Omega}$ on the boundary ∂Ω. To reach a divergence-free field , the boundary conditions must be specified in a manner to satisfy $\nabla\,.\,\boldsymbol{u}=0$ on the boundary. As a straightforward result of the corollary 1, this fact can be inferred that the divergence of the velocity field can be regulated by its boundary extremum values.

With regard to discrepancy between the vorticity, $\boldsymbol{\omega}$, and the curl of the velocity field, $\boldsymbol{u}$, there is a similar situation as mentioned above. Taking the curl of the Poisson Eq. (8), along with considering the identity $\Delta\boldsymbol{\omega}=\nabla(\nabla\,.\,\boldsymbol{\omega})-\nabla\times(\nabla\times\boldsymbol{\omega})$ and the fact that $\nabla\,.\,\boldsymbol{\omega}=0$, gives

$$\Delta(\nabla\times\boldsymbol{u}-\boldsymbol{\omega})=0\,, \tag{11}$$

https://doi.org/10.1017/jmech.2014.82 Published online by Cambridge University Press

where $\nabla \times \boldsymbol{u} - \boldsymbol{\omega}$ as a harmonic function can be a constant over the closure domain or else attains its maximum values on the boundaries. Hence, the discrepancy between the vorticity and curl of the velocity field can be controlled by its boundary values.

2.3 Retrieving the Vorticity Field and Constituting an Immersed Boundary

Consider a computational domain as shown in Fig. 1. This domain can include one or more solid subdomains Ω_s with moving or stationary boundaries Γ_s and a velocity source subdomain Ω_u which are surrounded by quiescent fluid domain Ω_f. Physical domain may be irregular and it can be extended to the computational domain with regular boundaries. This extension, from physical boundary Γ_B to computational boundary Γ_D may produce a marginal zone B. This extension causes the maximum values of divergence to be transferred to the computational boundary Γ_D, instead of physical boundary Γ_B. The solution in this region will be discarded from the ultimate solution. In problems with solid walls and no-slip boundary conditions, this technique works properly.

When a fluid system comprising one or more rigid structure, the Eq. (2) can be rewritten using the definition of the level set function as

$$\partial_t \boldsymbol{u} + \boldsymbol{u} \,.\, \nabla \boldsymbol{u} = -\nabla p + (1-\phi_s)[\nu \Delta \boldsymbol{u} + \boldsymbol{f}_f] + \phi_s \boldsymbol{f}_s, \quad \boldsymbol{x} \in \Omega, \tag{12}$$

where $\boldsymbol{f}_s$ and $\boldsymbol{f}_f$ are the body forces per unit of mass in solid and fluid phases, respectively. In this equation, ϕ_s denotes the level set function which is introduced as

$$\phi_s(\boldsymbol{x}) = \begin{cases} 1 & \text{for } \boldsymbol{x} \in \Omega_s, \\ 0 & \text{for } \boldsymbol{x} \in \Omega_f, \end{cases} \tag{13}$$

that means that the level set function takes the value 1 and 0 in the solid and fluid domain, respectively. To track the position of the solid structure, the evolution equation of the level set function is considered as

$$\partial_t \phi_s + \boldsymbol{u} \,.\, \nabla \phi_s = 0, \quad \boldsymbol{x} \in \Omega. \tag{14}$$

The Eqs. (3), (12) and (14) constitute the governing equations of the fluid-rigid structure interaction problems in primitive variables form. To express these equations in the form of the secondary variables, which is the velocity-vorticity formulation as the purpose of this paper, one can take the curl of the Eq. (12) and use the Eq. (8) as its complementary. The evolution equation of the level set function will remain unchanged. Therefore the following equations constitute the governing equations of the fluid-rigid structure interaction in the velocity-vorticity formulation in a special methodology which is the purpose of this paper.

$$\partial_t \boldsymbol{\omega} + \boldsymbol{u} \,.\, \nabla \boldsymbol{\omega} = \boldsymbol{\omega} \,.\, \nabla \boldsymbol{u} + (1-\phi_s)\, \nu \Delta \boldsymbol{\omega} + \nabla \times \left(\phi_s (\boldsymbol{f}_s - \boldsymbol{f}_f)\right), \quad \boldsymbol{x} \in \Omega \tag{15}$$

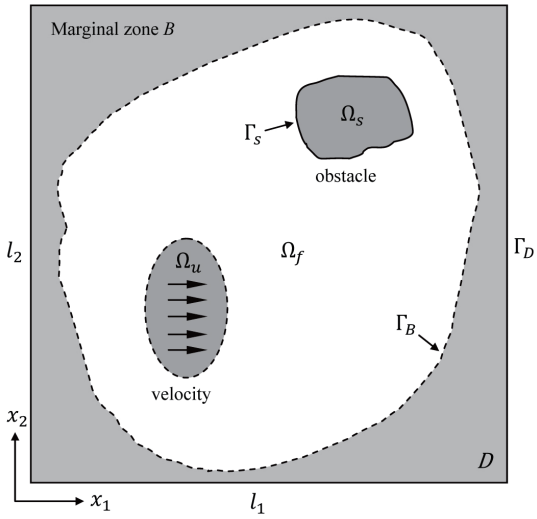


Fig. 1 Configuration of computational domain in immersed boundary method.

$$\Delta \boldsymbol{u} = -\nabla \times \boldsymbol{\omega}, \quad \boldsymbol{x} \in \Omega, \tag{16}$$

$$\partial_t \phi_s + \boldsymbol{u} \,.\, \nabla \phi_s = 0, \quad \boldsymbol{x} \in \Omega \tag{17}$$

what distinguishes the methodology of solving the problem from the conventional immersed boundary methods, how to apply the solid velocity in the fluid velocity field.

The algorithm of the proposed immersed boundary method based on the velocity-vorticity formulation is shown in Fig. 2. The procedure begins with initial vorticity field ω^0, initial level set function distribution ϕ_s^0 and known velocity boundary conditions $\boldsymbol{u}^{\partial\Omega}$. Then the kinematic relation for velocity-vorticity, Eq. (16), is solved to obtain the velocity field. Since the immersed boundaries are not included in the velocity calculation, it is expected that the velocity field does not satisfy the flow physics. Therefore, the next step should be devoted to apply the velocity immersed boundaries $\boldsymbol{u}^{IB}$. Depending on the type of the fluid-rigid structure problem, there are different strategies to apply the velocity of the rigid structure domain to the fluid velocity field. Some times a fixed rigid structure mimics the fluid flow field. Hence, the velocity of the immersed body $\boldsymbol{u}^{IB}$ sets to zero where the solid phase exists. In mathematical statement one can write

$$\boldsymbol{u}(\Omega_s) = \boldsymbol{u}^{IB}, \forall \boldsymbol{x} \,|\, \phi_s(\boldsymbol{x}, t^n) \geq 0.5, \tag{18}$$

where $\boldsymbol{u}^{IB} = 0$.

In the case of moving structures with predetermined motion equation, the velocity and position of the structure is known at any instant of time. Thus $\boldsymbol{u}^{IB}$ in Eq. (18) sets to $\boldsymbol{u}_s(t)$ which is the predetermined velocity of the structure domain.

There is a slightly different proposition in the case of mutual interaction of fluid-rigid structure, when one want to apply the velocity to the structure domain. To apply the velocity of the structure domain at the current

https://doi.org/10.1017/jmech.2014.82 Published online by Cambridge University Press

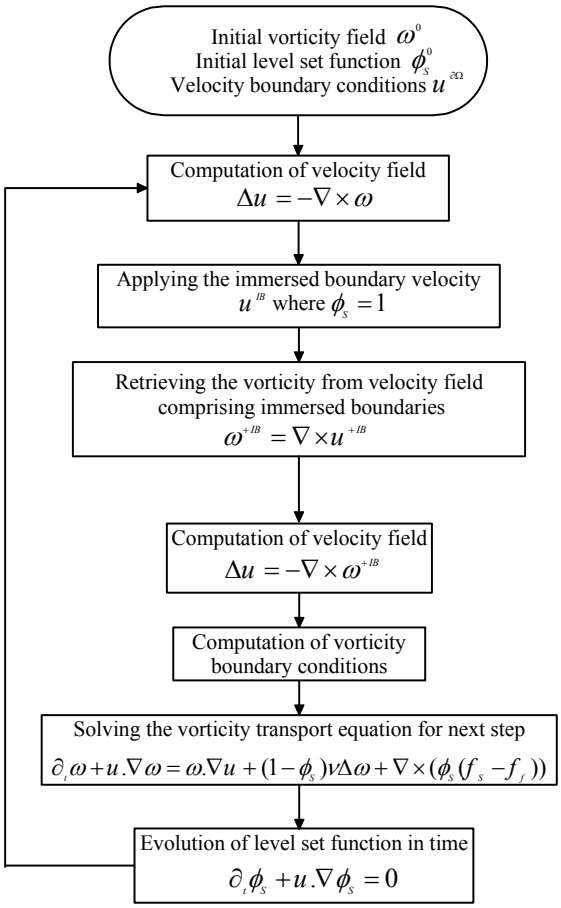


Fig. 2 Proposed algorithm of force free immersed boundary method.

time to the flow field, the velocity at the previous time step of the current position can be set to the structure domain. Hence,

$$\boldsymbol{u}(\Omega_s) = \boldsymbol{u}(\boldsymbol{x}, t^{n-1}) \,, \forall \boldsymbol{x} \,|\, \phi_s(\boldsymbol{x}, t^n) \geq 0.5 \,. \tag{19}$$

Because the structure domain is rigid, purpose of this study, an average velocity must be set to the structure domain as

$$\boldsymbol{u}(\Omega_s) = \overline{\boldsymbol{u}}(\boldsymbol{x}, t^{n-1}) = \frac{\sum_{i=1}^{N} \boldsymbol{u}(\boldsymbol{x}_i, t^{n-1})}{N} \,, \forall \boldsymbol{x}_i \,|\, \phi_s(\boldsymbol{x}_i, t^n) \geq 0.5 \,, \tag{20}$$

where N is the number of discrete points inside the structure domain.

According to the definition, $\boldsymbol{\omega} = \nabla \times \boldsymbol{u}$, vorticity field should be retrieved from the new velocity field $\boldsymbol{u}^{+IB}$, that is $\boldsymbol{u} \cup \boldsymbol{u}^{IB}$, contains the immersed structure domain velocity. Then the modified vorticity field $\boldsymbol{\omega}^{+IB}$ is used in the second kinematic relation of velocity-vorticity to obtain the physical velocity field. In the next step, vorticity boundary conditions are determined based on the physical velocity values which is derived from the second velocity-vorticity kinematic relation. The vorticity field at the next time step is calculated using the vorticity transport equation.

The next step is devoted to time integration of the level set function in the evolution Eq. (17). When a fixed structure mimics the flow field, the level set function does not change in time; hence, in Eq. (17) $\partial_t \phi_s = 0$ and correspondingly $\boldsymbol{u}.\nabla \phi_s = 0$. Since the velocity field is not zero everywhere, so the gradient of the level set function is zero. This means that the spatial distribution of the level set function in time is fixed and is equal to its initial conditions.

In the case of moving structure with predetermined motion, Eq. (17) can be rewritten as

$$\partial_t \phi_s + \boldsymbol{u}_s.\nabla\phi_s = 0 \tag{21}$$

where $\boldsymbol{u}_s$ is the velocity of the rigid structure. In a situation that the structure domain has not a predetermined motion, specifically in two-way interaction problems, the level set function takes a distribution troughout the solution domain and Eq. (17) takes the following form to convect the structure domain to the new position in the solution field, that is

$$\partial_t \phi_s + \overline{\boldsymbol{u}} \,.\nabla\phi_s = 0 \,, \tag{22}$$

where $\overline{\boldsymbol{u}}$ is the average velocity inside the rigid structure domain which is defined in Eq. (20).

The next section is devoted to examples, each of which represents a particular type of fluid structure interaction problems.

3. NUMERICAL EXPERIMENTS

In the current section the temporal and spatial convergence of the presented immersed boundary method is investigated with evaluating the accuracy and velocity divergence distribution. Hence, the flow between two concentric hollow cylinders is considered and its analytical solution is used as a criterion for comparison. In the case of the moving boundaries, the vortex shedding from the oscillating circular cylinder is studied. Falling a two dimensional cylinder in a quiescent fluid as a typical problem of the two-way fluid-structure interaction is investigated. Also, flow within the lid-driven cavity with interior cylindrical obstacles is considered to qualitatively validate the proposed method in steady-state flow.

3.1 Circular Couette Flow

The steady Couette flow between two concentric hollow cylinders is simulated. The domain of the solution is the square of the size [–1.25, 1.25] × [–1.25, 1.25] which comprises two concentric hollow cylinders with radii $r_i = 0.5$ and $r_o = 1$. The inner cylinder is rotated with angular velocity $\prod_i = 1$, and the outer cylinder is held stationary, $\prod_o = 0$. The configuration of the simulation domain consists of two concentric hollow cylinders is shown in Fig. 3. A uniform Cartesian grid is applied and L_2 and L_∞ norm of the exact error of the x-component of velocity are evaluated. The analytical solution of the steady state of this flow is given by

https://doi.org/10.1017/jmech.2014.82 Published online by Cambridge University Press

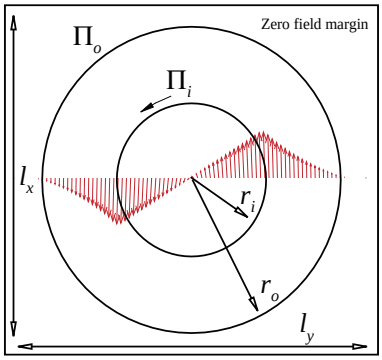


Fig. 3 Configuration of the simulation domain for the flow between two concentric cylinder (inner cylinder rotates and outer is stationary).

$$u = -\left(A + \frac{B}{r^2}\right) y\,, \tag{23}$$

$$v = \left(A + \frac{B}{r^2}\right) x\,, \tag{24}$$

where $r^2 = x^2 + y^2$, and A and B are

$$A = \frac{-\Pi_i\, r_i^2}{r_o^2 - r_i^2}\,, \tag{25}$$

$$B = \frac{\Pi_i\, r_i^2 r_o^2}{r_o^2 - r_i^2}\,. \tag{26}$$

The temporal resolution of the solution is regulated by the viscous CFL number

$$CFL = \frac{\delta t}{Re}\left(\frac{1}{\delta x^2} + \frac{1}{\delta y^2}\right). \tag{27}$$

Spatial and temporal convergence of the method is assayed with employing the several grid and time resolutions. Spatial convergence analysis was conducted based on Re = 10 and the results in Fig. 4(a) indicate that the rate of decay for the spatial errors of x-component of velocity to be 1.5 and about 2.8 in the L_∞ and the L_2 sense, respectively. The rate of decay for the temporal errors of x-component of velocity is also obtained in Fig. 4(b) as 1 for the L_∞ and 1.34 for the L_2. Due to the symmetry, similar results are obtained for the y-component of velocity.

The distribution of the x-component of velocity and the velocity divergence are shown in Fig. 5. The divergence field gives its maximum and minimum values of order 10^{-3} on the boundary. With the move towards the center of the solution domain, the divergence values are reduced significantly. This can be clearly observed in Fig. 5. Thus, in the region between the two cylinders, where the flow physics is important, the divergence of the velocity is reduced remarkably. The results of these comparisons and the spatial and temporal convergence rate of error norms show the ability of this method dealing with problems with curved and moving boundaries.

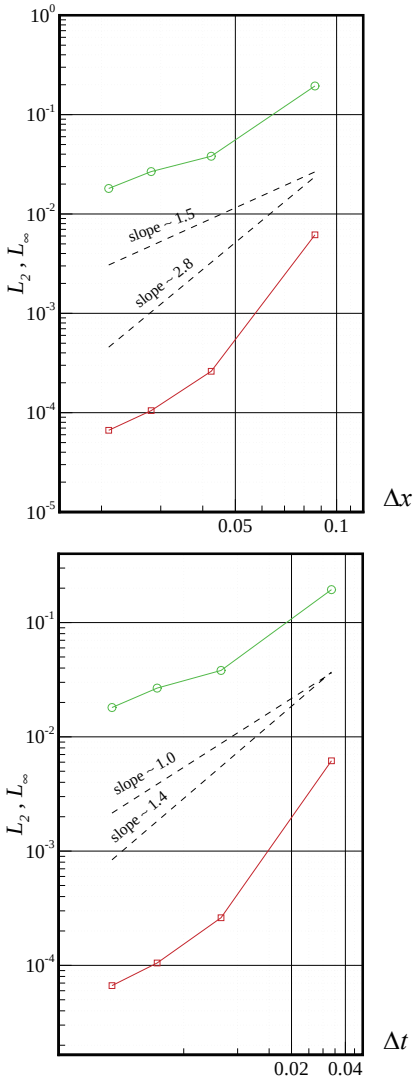


Fig. 4 Error norms L_∞ —○— and L_2 —□— of x-component of velocity versus spatial (top) and temporal (bottom) resolutions.

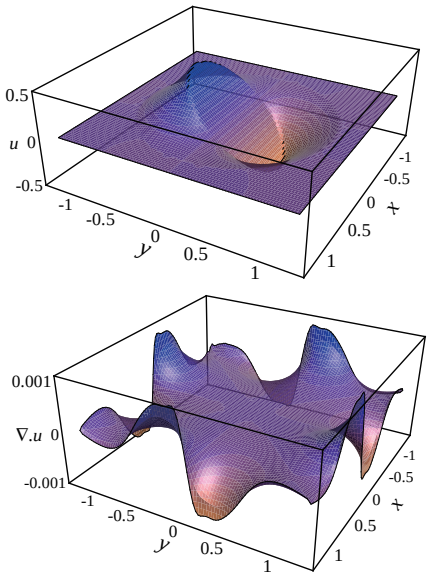


Fig. 5 Distribution of x-component of velocity (top) and velocity divergence (bottom).

https://doi.org/10.1017/jmech.2014.82 Published online by Cambridge University Press

3.2 In-Line Oscillating Cylinder in Quiescent Fluid

The oscillation of a circular cylinder in a quiescent fluid has investigated frequently in the literature [22,29-31]. This flow concerns two dimensionless parameters, *i.e.*, the Reynolds number, $\mathrm{Re} = U_{\max}D / \nu$ and Keulegan-Carpenter number, $KC = U_{\max} / fD$, where $U_{\max}$ and f are maximum velocity and characteristic frequency of the cylinder, respectively. Motion of the cylinder is predetermined by

$$x_c(t) = -\frac{1}{2\pi}\sin(2\pi ft)\,, \tag{28}$$

where x_c indicates the location of the cylinder center. The Reynolds number and Keulegan-Carpenter numbers are set to 100 and 5, respectively. The computational domain is a square of the size $20D$ in both directions consists a circular cylinder which is initially located in the center of the domain. The computational domain is discretized to a uniform grid of 400 × 400 cells and CFL number is about 0.18 based on Eq. (27). The simulation is started in a fluid at rest, and the cylinder oscillates according to Eq. (28) until periodic vortex shedding is established. Vorticity isolines at four phase angles of oscillation after beginning the vortex shedding are shown in Fig. 6. In the leftward motion, boundary layer develops on the leading face and separates at positions downstream, symmetrically. When the flow separates, two counter-rotating vortices are produced and persist until the rightward motion of the cylinder begins and subsequently the same vortex structure is created on the opposite side of the cylinder. The vortex pairs which are produced in each leftward (rightward) motion are split by the cylinder in its subsequent rightward (leftward) motion. The results are in good agreement with the corresponding numerical and laboratory experiments of Yang and Balaras [31] and Dutsch *et al.* [32], respectively, which indicates that the present method has succeeded to capture the qualitative features of the vorticity field dynamics.

A comparison is also performed between the velocity profiles at four x locations in three phases of oscillation in the current study and those numerical and experimental data which are extensively presented in the literature. The symmetric and anti-symmetric distribution of the u and v velocities along the y axis is shown in Fig. 7 which are in good agreement with the numerical data of [31,32].

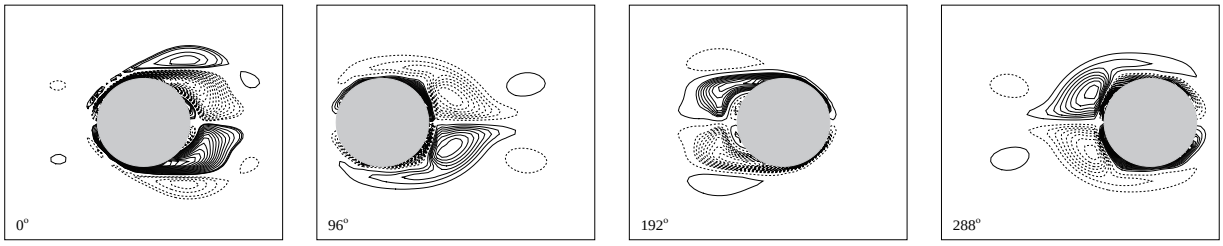


Fig. 6 Vorticity isolines at four phase of oscillation. Dashed and solid lines indicate the negative and positive values, respectively.

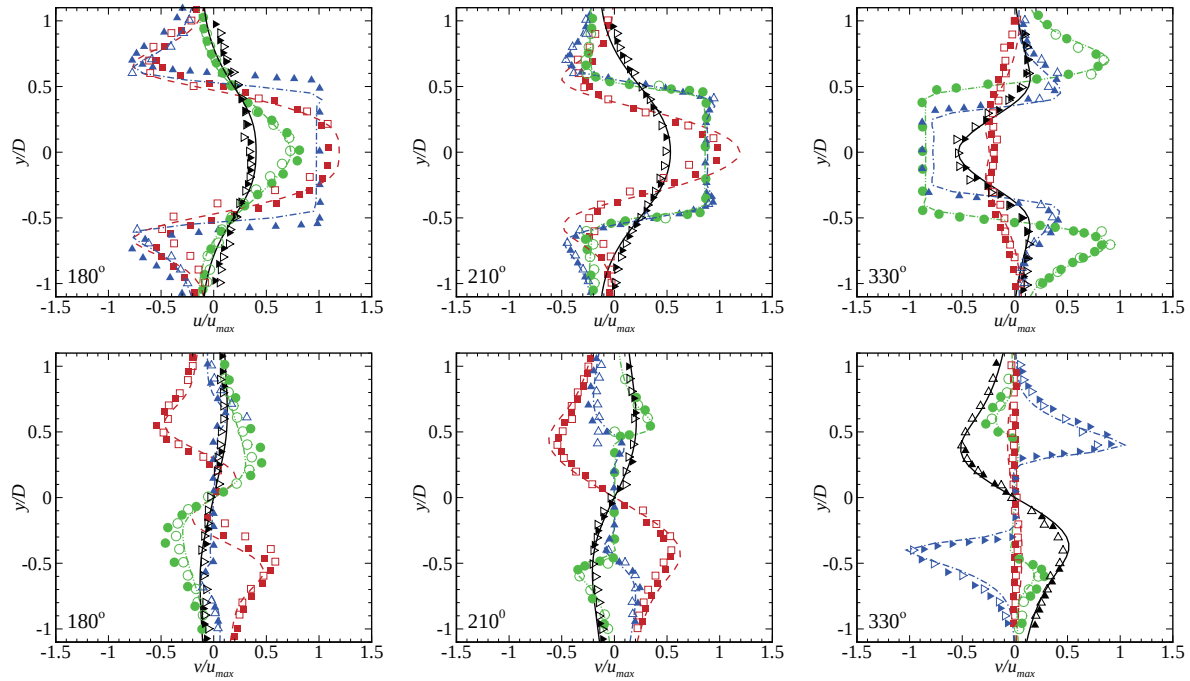


Fig. 7 The velocity profiles u (top) and v (bottom) at four x locations in three phases of oscillation, that is $x = -0.6D$ (– –, □■), $x = 0.0D$ (– · –, △▲), $x = 0.6D$ (– ·· –, ○●) and $x = 1.2D$ (—, ▷▶). The hollow and solid symbols correspond to the numerical and experimental data of [31,32], respectively.

https://doi.org/10.1017/jmech.2014.82 Published online by Cambridge University Press

In Fig. 8 the distribution of velocity divergence for four phases of oscillation is shown. It is well known that the velocity divergence in the midst of the solution domain, where the cylinder swings have been removed and this shows that physics of flow is satisfied.

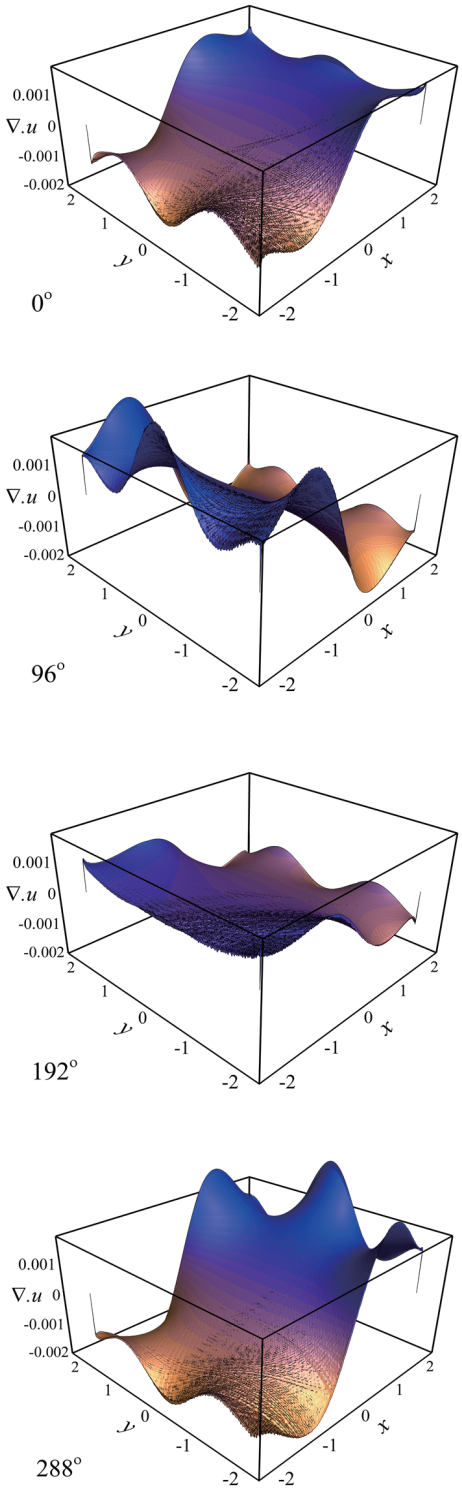


Fig. 8 The velocity divergence distribution in four phases of oscillation.

3.3 Falling a Two Dimensional Cylinder in Quiescent Fluid

The sedimentation of a two dimensional cylinder under gravity in a cavity containing a quiescent fluid is studied to indicate the capability of the presented method in the case of moving bodies which have not predetermined motion. This test serves as a way to validate the force calculations as a determinant factor. The same configuration and flow parameters are considered as those presented in the literature [33-35]. The dimension of the cavity is [0,2]m × [0,8]m, the viscosity is 0.01kg/(m.s), the density inside and outside the cylinder is 1.5 and 1.0kg/m^3. The cylinder has radius 0.125m and is initially located at the point (1m, 4m). The cylinder is accelerating under gravity, set to g =–980m/s^2, then reaches a steady velocity, due to the viscous forces, and eventually hit the bottom of the cavity and stops. In this study the contact and rebound problems are left for our future studies.

The governing equations, Eq. (15) ~ (17), are discretized on a fixed cartesian grid. A second order central difference approximation is used for spatial discretizing the viscous diffusion terms and lagging linearization method is applied for spatial discretizing the convective terms. The other spatial derivatives are discretized with second order central difference approximation for midpoints of the solution domain and forward and backward schemes for the boundary points. The full multigrid (FMG) method, with red-black Gauss-Seidel as the smoothing operator, is used for solving the Poisson's Eq. (16). The grid independency is checked for three resolutions 129 × 513, 257 × 1025 and 513 × 2049. Integration in time to solve the vorticity transport equation is performed using a first-order Euler's method. A second-order two-step MacCormack method is used for integrating the level set function equation, Eq. (17). It should be emphasized that the simillar numerical scheme as mentioned above is employed in all numerical experiments. Since, this study is devoted to the behavior of a rigid body in the FSI, the level set function in Eq. (17) must be advected by average velocity $\bar{\boldsymbol{u}}$, Eq. (20), instead of $\boldsymbol{u}$. In this simulation CFL number $\nu\Delta t / (\Delta x)^2$ is set to 0.0065. Figures 9(a) and 9(b) represents the fall velocity and vertical position changes versus time, respectively. Figure 9 shows that our results match almost perfectly those of Glowinski *et al.* [33] and Coquerelle and Cottet [34]. In the case of falling circular cylinder, it should be noted that the cylinder travels a straight line and does not experience any transverse vibration. The contours of vorticity are also shown in Fig. 10. This is also found by Horowitz and Williamson [36] that falling cylinders, oriented horizontally, all descend in a rectilinear path.

3.4 A Lid-Driven Cavity Flow with Multiple Obstacles

The proposed method is also investigated with deriving and comparing the flow pattern in a lid-driven cavity containing five circular obstacles with those in

https://doi.org/10.1017/jmech.2014.82 Published online by Cambridge University Press

literature [37,38]. The numerical simulation is performed in a cavity with square domain [−1,1] × [−1,1], consists of five circular obstacles of radius 0.15 and centered at (0, 0), (0, ±0.6) and (±0.6, 0). The flow inside the cavity is induced by horizontal velocity along the upper boundary, that is $u = 1.0$. No-slip boundary conditions are applied along the other sides of the cavity. The mesh size is 201 × 201, and the Reynolds number is 100 based on the lid-driven velocity and the height of the cavity. Temporal step is chosen as 0.001 which results in CFL number 0.2. Figure 11 shows how the obstacles mimic the cavity flow pattern. This steady flow pattern have qualitatively excellent agreement with those represented in [37,38].

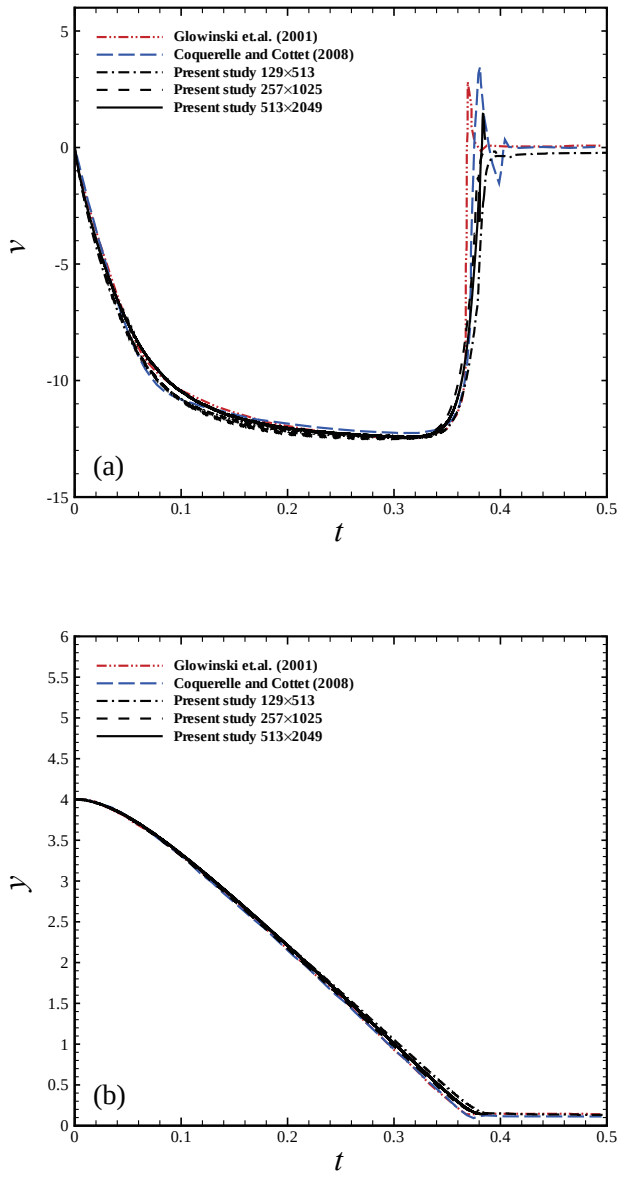


Fig. 9 Plots of (a) fall velocity and (b) vertical position versus time for three grid resolutions compared with results of Glowinski *et.al.* [33], Coquerelle and Cottet [34].

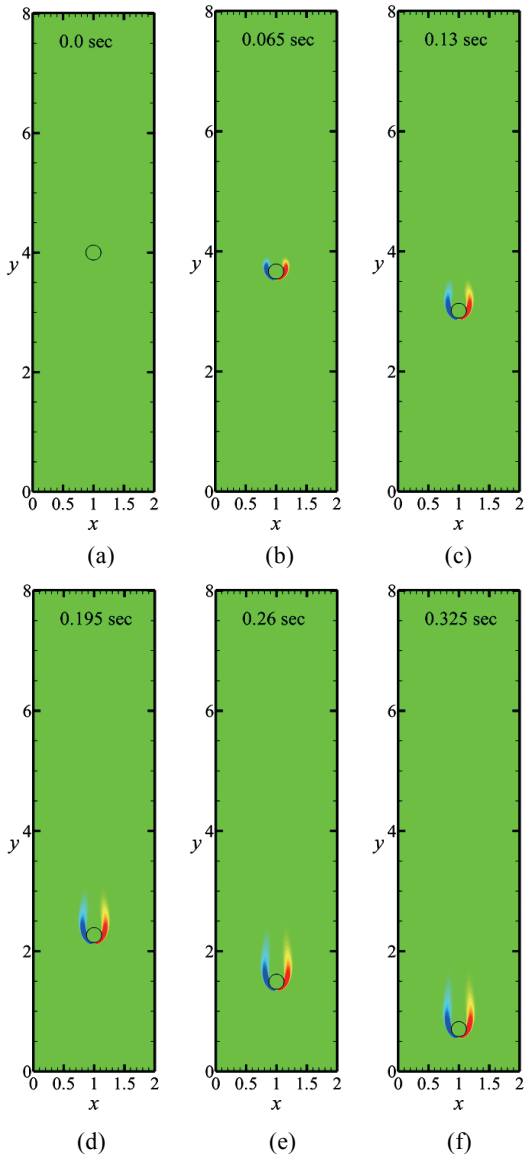


Fig. 10 The contours of vorticity around the falling cylinder at various times.

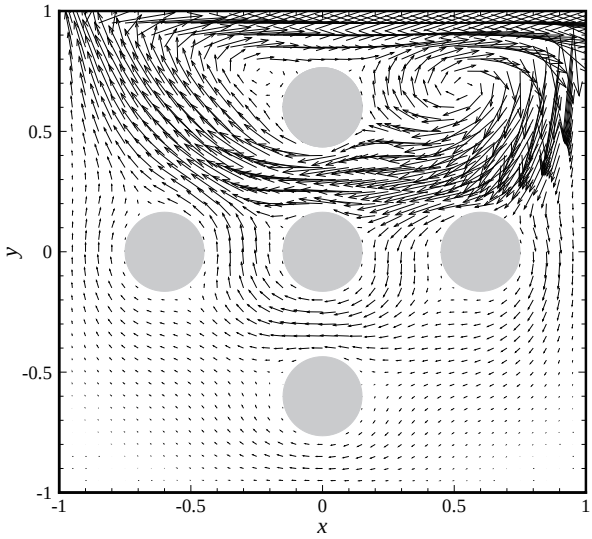


Fig. 11 The cavity flow pattern affected by five circular obstacles at Reynolds 100.

https://doi.org/10.1017/jmech.2014.82 Published online by Cambridge University Press

4. CONCLUSIONS

We have presented an explanation of velocity-vorticity formulation in the finite-difference framework to define a new immersed boundary method which not any more needs to calculation of force term. The kernel of the method was retrieving the vorticity field from the velocity field and recalculating the velocity using the vorticity field comprises the immersed boundaries. The method showed the excellent results in the case of one and two-way coupling of a fluid with rigid bodies. In the current study, the effect of the rigid bodies on the flow field was merely investigated and one example (falling a two dimensional cylinder in a quiescent fluid) was devoted to mutual interaction of fluid and structure. To verify the results we have resorted to the test case of circular Couette flow with analytical solution. the temporal and spatial convergence test indicated the acceptable rate of error reduction based on L_∞ and L_2 definition. The numerical experiments illustrated that the velocity field near the immersed boundaries becomes approximately divergence free. This issue was clearly shown in Fig. (5) in steady state and in Fig. (8) at four phases of oscillation. Since the focus of this paper is on the new numerical method, we thus present numerical results for a few problems without too much elaborations about their physical meanings. This was also qualitatively illustrated in Fig. (11) that the method is proper when several bodies mimic the flow field. In the present method, the complexities due to applying the direct forcing at the immersed boundaries, are resolved by retrieving the vorticity field from the velocity field. The main disadvantage of the proposed method is duplicate solution of the velocity Poisson's equations. To remedy this problem the full multigrid (FMG) method is suggested to solve the Poisson's equations which considerably reduces the computing time. The next work will be devoted to model the mutual interaction of the fluid and rigid structures in details, using the proposed immersed boundary method.

ACKNOWLEDGMENTS

The authors would like to express their sincere appreciation for respectable editor Dr. J. T. Chen, who directs this paper to be presented in the best status. The authors also thank the reviewers for their fruitful comments and directions.

REFERENCES

1. Quartapelle, L., "Numerical Solution of the Incompressible Navier-Stokes Equations," *International Series of Numerical Mathematics, Birkhäuer-Verlag, Basel*, **133** (1993).
2. Rempfer, D., "On Boundary Conditions for Incompressible Navier-Stokes Problems," *Applied Mechanics Reviews*, **59**, pp. 107–125 (2006).
3. Ferziger, J. H., "Simulation of Incompressible Turbulent Flows," *Journal of Computational Physics*, **69**, pp. 1–48 (1987).
4. Peyret, R. and Taylor, T. D., *Computational Methods for Fluid Flow*, Springer-Verlag, Berlin (1983).
5. Sabetghadam, F., Sharafatmandjoor, S. and Badri, M., "Construction of Solenoidal Immersed Velocity Vectors Using the Kinematic Velocity-Vorticity Relation," arXiv: 1204.1916, http://arxiv.org/abs/1204.1916 (2012).
6. Glowinski, R., Pan, T. W., Hesl, T. I. and Joseph, D. D., "A Distributed Lagrange Multiplier/Fictitious Domain Method for Particulate Flows," *International Journal of Multiphase Flow*, **25**, pp. 755–794 (1999).
7. Sussman, M., Smereka, P. and Osher, S., "A Level Set Approach for Computing Solutions to Incompressible Two-Phase Flows," *Journal of Computational Physics*, **114**, pp. 146–159 (1994).
8. Tryggvason, G., Bunner, B., Esmaeeli, A., Juric, D., Al-Rawahi, N., Tauber, W., Han, J., Nas, S. and Jan, Y. J., "A Front-Tracking Method for the Computations of Multiphase Flow," *Journal of Computational Physics*, **169**, pp. 708–759 (2001).
9. Huang, W. X. and Sung, H. J., "An Immersed Boundary Method for Fluid-Flexible Structure Interaction," *Computer Methods in Applied Mechanics and Engineering*, **198**, pp. 2650–2661 (2009).
10. Wang, Z., Fan, J. and Cen, K., "Immersed Boundary Method for the Simulation of 2D Viscous Flow Based on Vorticity-Velocity Formulations," *Journal of Computational Physics*, **228**, pp. 1504–1520 (2009).
11. Peskin, C. S., "Flow Patterns Around Heart Valves: A Numerical Method," *Journal of Computational Physics*, **10**, pp. 252–271 (1972).
12. Fadlun, E. A., Verzicco, R., Orlandi, P. and Mohd-Yusof, J., "Combined Immersed-Boundary Finite-Difference Methods for Three-Dimensional Complex Flow Simulations," *Journal of Computational Physics*, **161**, pp. 35–60 (2000).
13. Kim, J., Kim, D. and Choi, H., "An Immersed-Boundary Finite-Volume Method for Simulations of Flow in Complex Geometries," *Journal of Computational Physics*, **171**, pp. 132–150 (2001).
14. Griffith, B. E., "Simulating the Blood-Muscle-Valve Mechanics of the Heart by an Adaptive and Parallel Version of the Immersed Boundary Method," Ph.D. Dissertation, Courant Institute of Mathematical Sciences, New York University, New York, US (2005).
15. Kim, Y. and Peskin, C. S., "Penalty Immersed Boundary Method for an Elastic Boundary with Mass," *Physics of Fluids*, **19**, pp. 1–18 (2007).
16. Le, D. V., Khoo, B. C. and Lim, K. M., "An Implicit-Forcing Immersed Boundary Method for Simulating Viscous Flows in Irregular Domains," *Computer Methods in Applied Mechanics and Engineering*, **197**, pp. 2119–2130 (2008).

https://doi.org/10.1017/jmech.2014.82 Published online by Cambridge University Press

17. Poncet, P., "Analysis of an Immersed Boundary Method for Three-Dimensional Flows in Vorticity Formulation," *Journal of Computational Physics*, **228**, pp. 7268–7288 (2009).
18. Bonfigli, G., "High-Order Finite-Difference Implementation of the Immersed-Boundary Technique for Incompressible Flows," *Computer & Fluids*, **46**, pp. 2–11 (2011).
19. Ren, W. W., Wu, J., Shu, C. and Yang, W. M., "A Stream Function-Vorticity Formulation-Based Immersed Boundary Method and its Applications," *International Journal for Numerical Methods in Fluids*, **70**, pp. 627–645 (2012).
20. Wu, C. S. and Young, D. L., "Simulations of Free-Surface Flows with an Embedded Object by a Coupling Partitioned Approach," *Computer & Fluids*, **89**, pp. 66–77 (2014).
21. Uhlmann, M., "An Immersed Boundary Method with Direct Forcing for the Simulation of Particulate Flows," *Journal of Computational Physics*, **209**, pp. 448–476 (2005).
22. Kim, D. and Choi, H., "Immersed Boundary Method for Flow Around an Arbitrarily Moving Body," *Journal of Computational Physics*, **212**, pp. 662–680 (2006).
23. Huang, W. X., Shin, S. J. and Sung, H. J., "Simulation of Flexible Filaments in a Uniform Flow by the Immersed Boundary Method," *Journal of Computational Physics*, **226**, pp. 2206–2228 (2007).
24. Zhao, H., Freund, J. B. and Moser, R. D., "A Fixed-Mesh Method for Incompressible Flow-Structure Systems with Finite Solid Deformations," *Journal of Computational Physics*, **227**, pp. 3114–3140 (2008).
25. Le, D. V., White, J., Peraire, J., Lim, K. M. and Khoo, B. C., "An Implicit Immersed Boundary Method for Three-Dimensional Fluid-Membrane Interactions," *Journal of Computational Physics*, **228**, pp. 8427–8445 (2009).
26. Curet, O. M., AlAli, I. K., MacIver, M. A. and Patankar, N. A., "A Versatile Implicit Iterative Approach for Fully Resolved Simulation of Self-Propulsion," *Computer Methods in Applied Mechanics and Engineering*, **199**, pp. 2417–2424 (2010).
27. Herschlag, G. and Miller, L., "Reynolds Number Limits for Jet Propulsion: A Numerical Study of Simplified Jellyfish," *Journal of Theoretical Biology*, **285**, pp. 84–95 (2011).
28. Chaudhuri, A., Hadjadj, A. and Chinnayya, A., "On the Use of Immersed Boundary Methods for Shock/Obstacle Interactions," *Journal of Computational Physics*, **230**, pp. 1731–1748 (2011).
29. Choi, J. I., Oberoi, R. C., Edwards, J. R. and Rosati, J. A., "An Immersed Boundary Method for Complex Incompressible Flows," *Journal of Computational Physics*, **224**, pp. 757–784 (2007).
30. Liao, C. C., Chang, Y. W., Lin, C. A. and McDonough, J. M., "Simulating Flows with Moving Rigid Boundary Using Immersed-Boundary Method," *Computer & Fluids*, **39**, pp. 152–167 (2010).
31. Yang, J. and Balaras, E., "An Embedded-Boundary Formulation for Large-Eddy Simulation of Turbulent Flows Interacting with Moving Boundaries," *Journal of Computational Physics*, **215**, pp. 12–40 (2006).
32. Dutsch, H., Durst, F., Becker, S. and Lienhart, H., "Low-Reynolds-Number Flow Around an Oscillating Circular Cylinder at Low Keulegan-Carpenter Numbers," *Journal of Fluid Mechanics*, **360**, pp. 249–271 (1998).
33. Glowinski, R., Pan, T. W., Hesla, T. I., Joseph, D. D. and Périauxz, J., "A Fictitious Domain Approach to the Direct Numerical Simulation of Incompressible Viscous Flow Past Moving Rigid Bodies: Application to Particulate Flow," *Journal of Computational Physics*, **169**, pp. 363–426 (2001).
34. Coquerelle, M. and Cottet, G. H., "A Vortex Level Set Method for the Two-Way Coupling of an Incompressible Fluid with Colliding Rigid Bodies," *Journal of Computational Physics*, **227**, pp. 9121–9137 (2008).
35. Bergmann, M. and Iollo. A., "Modeling and Simulation of Fish-Like Swimming," *Journal of Computational Physics*, **230**, pp. 329–348 (2011).
36. Horowitz, M. and Williamson, C. H. K., "Vortex-Induced Vibration of a Rising and Falling Cylinder," *Journal of Fluid Mechanics*, **662**, pp. 352–383 (2010).
37. Ito, K., Lai, M. C. and Li, Z., "A Well-Conditioned Augmented System for Solving Navier-Stokes Equations in Irregular Domains," *Journal of Computational Physics*, **228**, pp. 2616–2628 (2009).
38. Su, S. W., Lai, M. C. and Lin, C. A., "An Immersed Boundary Technique for Simulating Complex Flows with Rigid Boundary," *Computer & Fluids*, **36**, pp. 313–324 (2007).

(Manuscript received December 24, 2013,
accepted for publication June 22, 2014.)

https://doi.org/10.1017/jmech.2014.82 Published online by Cambridge University Press